LBL-35927
UC-401
Preprint

Lawrence Berkeley Laboratory

UNIVERSITY OF CALIFORNIA

CHEMICAL SCIENCES DIVISION

Submitted to Journal of Chemical Physics

Photodissociation Dynamics of the Methyl Radical 3s Rydberg State

S. North, D.A. Blank, P. Chu, and Y.T. Lee

July 1994

REFERENCE COPY
Does Not
Circulate
Bldg. 50 Library.
LBL-35927
Copy 1

Prepared for the U.S. Department of Energy under Contract Number DE-AC03-76SF00098

DISCLAIMER

This document was prepared as an account of work sponsored by the United States Government. While this document is believed to contain correct information, neither the United States Government nor any agency thereof, nor the Regents of the University of California, nor any of their employees, makes any warranty, express or implied, or assumes any legal responsibility for the accuracy, completeness, or usefulness of any information, apparatus, product, or process disclosed, or represents that its use would not infringe privately owned rights. Reference herein to any specific commercial product, process, or service by its trade name, trademark, manufacturer, or otherwise, does not necessarily constitute or imply its endorsement, recommendation, or favoring by the United States Government or any agency thereof, or the Regents of the University of California. The views and opinions of authors expressed herein do not necessarily state or reflect those of the United States Government or any agency thereof or the Regents of the University of California.

Photodissociation Dynamics of the Methyl Radical 3s Rydberg State

Simon North, David A. Blank, Pamela Chu[1], and Yuan T. Lee

Chemical Sciences Division, Lawrence Berkeley Laboratory,
and
Department of Chemistry, University of California, Berkeley, CA 94720

1. Present Address: National Institute of Standards and Technology, Gaithersburg, MD.

Photodissociation Dynamics of the Methyl Radical 3s Rydberg State

Simon W. North, David A. Blank, Pamela Chu[1], and Yuan T. Lee
Chemical Sciences Division, Lawrence Berkeley Laboratory,
and
Department of Chemistry, University of California, Berkeley, CA 94720, USA

The photodissociation dynamics of methyl radical have been investigated at 193.3 nm using photofragment translational spectroscopy. The formation of CH_2 and $H(^2S)$ was the only dissociation pathway observed. Although it is not possible to assign the spin state of the methylene unambiguously, we believe that methylene is produced predominately in the a^1A_1 excited state. The translational energy distribution of the products is peaked at ~13 kcal/mole which is consistent with the magnitude of the exit barrier on the excited state potential energy surface. The breadth of the distribution suggests that the methyl radicals dissociate from a wide range of geometries. From the photofragment angular distribution an anisotropy parameter of β=-0.9±0.1 was determined.

I. Introduction

Although the ground state reactivity and decomposition of methyl radical have been the subject of numerous studies[1], there is little information regarding the photochemistry of even the lowest electronically excited state. In fact, there are only two reports which have *directly* detected a dissociation product arising from B-state photochemistry.[2,3] This is somewhat surprising in light of the considerable attention given to the analogous A-states of NH_3 and H_2O.[4]

The ultraviolet spectroscopy of the methyl radical was first examined by Herzberg and Shoosmith[5] and the transition originating at 216 nm was assigned to an excitation of the unpaired $2p_z$ electron to a 3s Rydberg orbital. The broadening of the CH_3 transition was attributed to a rapid predissociation of the excited state due to H-atom tunnelling.[6] Callear and Metcalfe subsequently resolved vibrational features between 216-204 nm beyond which the spectrum evolves into a broad continuum.[7] The transition at 193.3 nm, therefore, is an excitation not to a discrete band but an absorption to the *dissociative continuum*. Methyl radical photodissociation has been

1. Present Address: National Institute of Standards and Technology, Gaithersburg, MD.

observed at this wavelength as both a primary process[8] and as a secondary process in the dissociation of acetone[9] and azomethane.[10]

At 193.3 nm there are three energetically allowed dissociation pathways, two involving the loss of an H-atom and one involving the elimination of H_2. Orbital correlations in the dissociation of the methyl radical were first examined theoretically by Yu *et al.*[4] In agreement with the earlier postulation of Herzberg, the B-state was found to correlate with the formation of singlet methylene, $CH_2(a^1A_1)$,

$$CH_3(B^2A_1') \text{----------}> CH_2\,(a^1A_1) + H\,(^2S) \qquad (1).$$

and the ground state methyl radicals correlate to two asymptotic dissociation channels,

$$CH_3(X^2A_2'') \text{----------}> CH_2\,(X^3B_1) + H\,(^2S) \qquad (2)$$

$$CH_3(X^2A_2'') \text{----------}> CH\,(X^2\Pi) + H_2\,(^1\Sigma_g^+) \qquad (3)$$

which are predicted to occur in comparable yields at vibrational energies corresponding to ~216 nm excitation followed by internal conversion.[2] Although the elimination of molecular hydrogen does not correlate with the $CH_3(B^2A_1')$ state along either C_{2v} or C_s-pyramidal pathways, C_s-planar or C_1 pathways are allowed. At 216 nm reaction 3 was inferred from OH fluorescence produced via the reaction of $CH(X^2\Pi)$ with O_2.[11] However, Ye *et al.* found that CH(A,B-X) fluorescence resulting from methyl radical photodissociation at 193.3 nm was quadratically dependent on the laser power.[8] The authors concluded that CH originated from the secondary dissociation of methylene implying that at 193.3 nm H_2 elimination does not compete efficiently with simple C-H bond cleavage. Only H-atom elimination from methyl radical photodissociation was considered by the authors of references 9 and 10. *Ab initio* calculations by Yu *et al.* predicted a barrier to dissociation of 11.5 kcal/mole at $R_{C\text{-}H}$=1.55 Å for reaction 1. It was noted, however, that the calculated barrier may be reduced to 4.6-9.2 kcal/mole with a more

substantial basis set and increased configuration interaction. Resonance Raman experiments carried out by Kelly and co-workers have addressed the ro-vibronic dependence of the predissociation lifetimes of the B-state.[12,13] J-dependent tunneling rates of the B-state origin band were modelled with a 1-dimensional cubic potential and a best fit to the experimental data yielded a barrier of 6.29 kcal/mole at R_{C-H}=1.38 Å.[13] Recent high level *ab initio* calculations performed by Botschwina *et al.* were in accord with the results of Kelly.[14] Figure 1 shows the energy level diagram for the photodissociation of methyl radical including correlations for a HCH angle of 120°.

Despite the theoretical work and spectroscopic measurements there have been few experimental investigations involving the photodissociation of the B-state. Chen *et al.* investigated the photochemistry of methyl radical at 216 nm and detected the CH_2 (*m/e*=14) photofragment by photoionization at 10.5 eV although the spin state of the methylene could not be assigned.[2] No *m/e*=13 (CH^+) product was observed but since the 10.5 eV photon lies below the CH($^2\Pi$, v=0) adiabatic ionization potential, determination of the branching ratio between H-atom and H_2 elimination was not possible. Recently, Dixon and co-workers measured H-atom time-of-flight from methyl radical photodissociation at 216 nm following CH_3SH photolysis.[3] Contrary to all theoretical predictions ground state methylene (X^3B_1) was determined to be the momentum matched fragment. This conclusion was based on energetic considerations *i.e.* there was insufficient energy available concomitant with the formation of $CH_2(a^1A_1)$ to account for the short arrival times of the observed H-atoms. It was postulated that the formation of triplet methylene resulted from a coupling between the ground and excited state potential energy surfaces in the exit channel at small CH_2 angles (~104°). The structure in the time-of-flight, originally thought to be CH_2 bending excitation, was later found to be inconsistent with the dissociation of CH_3.[15,16] These features have since been attributed to the photolysis of CH_3S arrising from the dissociation of CH_3SH.[17] A reinvestigation of methyl radical dissociation at 216 nm suggests that only $CH_2(a^1A_1)$ is produced in agreement with theoretical predictions.[15] The measured translational energy release however, *is energetically consistent with either singlet or triplet methylene.*

In this paper we present results on the photodissociation of methyl radical excited at 193.3 nm using photofragment translational spectroscopy. This is the only experiment which has directly measured the H-atom/H_2 elimination branching ratio at any wavelength. The only observed products were CH_2 and H. This is extremely relevant to those interested in the 193 nm photolysis of acetone and azomethane as a source of CH_3 for kinetics studies. Although our methodology cannot unambiguously discriminate between the different spin states of the methylene we believe, based on the translational energy and photofragment anisotropy, that the CH_2 photoproduct is formed predominantly in the a^1A_1 excited state.

II. Experimental

Two experimental configurations were used in this work. All of the photofragments, with the exception of H and H_2, were measured using a fixed-source rotatable-detector apparatus as described previously.[18,19] The pulsed beam of radicals was generated from the pyrolysis of a suitable precursor. Although both azomethane and di-*tert*-butyl peroxide (DTBP) were employed with similar success, all of the data presented in this paper was obtained with DTBP as the precursor. A pulsed valve[20] fitted with a SiC pyrolysis nozzle (1.0 mm I.D.) was operated at 80 Hz. The source employed is an adaptation of the one designed and characterized by Chen *et al.* and a more complete description can be found elsewhere.[21] Briefly, a SiC tube was resistively heated to ~1400 K, as determined from optical pyrometry and beam time-of-flight, by a DC current limited power supply. DTBP, <1%, was expanded in helium at a total stagnation pressure of ~800 torr. The thermal decomposition of DTBP results in two methyl radicals and two acetone molecules and has been shown to be an efficient source of CH_3.[22] Shown in Figure 2 are mass spectra of the molecular beam with the nozzle unheated (upper trace) and heated (lower trace). The lower spectra shows the quantitative loss of the parent (*m/e*=146, *m/e*=73, and *m/e*=57 etc.), the appearance of the known cracking pattern for acetone, and a large contribution from the methyl radical parent (*m/e*=15). The beam was measured *in situ* and had a velocity of ~3600 m/s with a FWHM of ~15%. The pulsed beam was twice collimated to an angular divergence of 2° and crossed at a right angle with the output of a Lambda-Physik EMG 202 MSC excimer laser which was operated

at the ArF transition (193.3 nm). The 5-30mJ/pulse output was focussed to a 2x4 mm spot in the interaction region using a spherical lens (f=30 cm). Polarization of the laser beam was achieved by 10 quartz plates at Brewster's angle (>95% polarization). The neutral photoproducts travelled 20.8 cm where they were ionized by electron bombardment and mass selected using a quadrupole mass filter. The ions were then counted as a function of time using a Daly ion counter and a multi-channel scaler interfaced to a computer that was triggered with the laser pulse.

In order to detect H and H_2 photofragments an alternative arrangement was necessary. The requirements for detection of these fragments have been thoroughly discussed elsewhere and will only be summarized.[23,24] The pulsed valve with pyrolytic nozzle was mounted mutually perpendicular to both the detector and the laser beam. The radicals were photolyzed ~4.0 mm above the nozzle opening and the H-atom photoproducts passed through two 3.0 mm skimmers 28.5 cm to the detector. Although the beam velocity distribution could not be determined in this configuration, the H-atom velocity is large compared to the beam velocity and as a result the H-atom TOF spectra were found to be relatively insensitive to the beam conditions. The data was fit with the forward convolution technique. Details of the fitting procedure and the data analysis program can be found elsewhere.[25]

The DTBP 98% was obtained from Aldrich and used without further purification. Azomethane was synthesized by the method of Renaud and Leitch[26] and was purified by trap to trap distillation prior to use.

III. Results and Analysis

Time-of-flight spectra (TOF) were taken at *m/e*=12-15, *m/e*=2, and *m/e*=1 with unpolarized light. TOF spectra of *m/e*=28 (CO^+) were also collected in order to confirm the photodissociation of acetone, a pyrolysis bi-product. Acetone is known to have an appreciable absorption cross section (~2.7×10^{-18} cm^2) at 193.3 nm due to a 3s Rydberg transition.[27] The dynamics of acetone photodissociation, particularly the resulting translational energy distributions of the CH_3 and CO photofragments, have been well characterized.[28,29] All of the observed signals exhibited a linear dependence upon the laser power demonstrating that the photofragments resulted exclu-

sively from single photon processes at the laser fluences employed. Time dependent background from the pulsed valve was collected with the laser off and subsequently subtracted from the TOF spectra. Figure 3 shows TOF spectra taken at Θ_{lab}=7.5° at *m/e*=15-12. The *m/e*=15 (CH_3^+) (Figure 3a) cannot arise from methyl radical photodissociation and was successfully fit, as shown by the solid line, with the previously determined translational energy distribution, $P(E_T)$, for the photodissociation of acetone at 193.3 nm.[28] TOF spectra at *m/e*=28 were also fit using the $P(E_T)$ for acetone photodissociation. In the *m/e*=14 (CH_2^+) TOF spectrum, in addition to the CH_3 daughter ion from acetone, is a second feature which appears at longer times. This is attributed to methylene originating from the photodissociation of methyl radical. An identical feature is observed at *m/e*=12-14 when using azomethane as the radical precursor and, therefore, the assignment of this peak can be made with some confidence.[30] The dashed line is the fit to the methylene contribution using the $P(E_T)$ shown in Figure 4. Any $CH(^2\Pi)$ produced from the elimination of H_2 would appear at *m/e*=13 (CH^+) and *m/e*=12 (C^+). Both of these spectra can be fit without including the CH + H_2 channel and therefore it appears that formation of CH_2 and H is the only active dissociation channel. Additional TOF spectra for *m/e*=12 at laboratory angles of 10° and 14° are shown in Figure 5.

A representative H-atom (*m/e*=1) TOF spectrum is shown in Figure 6 with the time dependent background subtracted. The solid line fit to the data is using the $P(E_T)$ obtained from fitting the CH_2 (*m/e*=14-12) TOF spectra demonstrating that this is the *momentum matched fragment.* Since H-atom elimination from both acetone[9] and azomethane[10] is thought to occur in minor yields at 193 nm the importance of measuring the momentum matching partner cannot be overemphasized in unambiguous determination of the dissociation channels. Similar *m/e*=1 TOF spectra were obtained in the pyrolysis of azomethane. Furthermore, lowering the temperature of the SiC nozzle >100°C eliminated the H-atom peak entirely. Shown in Figure 7 are laser on and laser off spectra at *m/e*=2, each accumulated for 2,000,000 shots. Within the signal-to-noise ratio of the data we conclude that there is no H_2 produced from the photodissociation of CH_3 at 193.3 nm. This is in agreement with the analysis above of the heavy fragments. Based on the heavy

fragment (*m/e*=15-12) and *m/e*=2 data we estimate that if the CH + H_2 channel exists it certainly represents <5% of the dissociation products.

The center-of-mass $P(E_T)$ shown in Figure 4 is peaked away from zero, $\langle E_T \rangle \sim 15$ kcal/mole, with a FWHM of 12 kcal/mole. The available energy for the formation of ground state methylene is given by,

$$E_{avail} = h\nu_{193nm} - D_o(H_2C\text{-}H) \qquad (4)$$

where $h\nu_{193nm}$ is the photon energy (147.8 kcal/mole) and $D_o(C\text{-}H)$ is the bond dissociation energy. From the known heats of formation for $CH_2(X^3B_1)$ (92.6 kcal/mole)[31], $H(^2S)$ (52.1 kcal/mole)[32], and $CH_3(X^2A_2'')$ (34.0 kcal/mole)[32] the C-H bond dissociation energy in CH_3 is 110.7 kcal/mole. Therefore, the available energy for production of $CH_2(X^3B_1)$ + H is 37.1 kcal/mole. The singlet-triplet splitting in CH_2 has been the subject of a voluminous literature.[33] Adopting the accepted best value of 9.08 kcal/mole the available energy for the formation of $CH_2(a^1A_1)$ + H is then, 147.8-110.7-9.08=28.0 kcal/mole.

Equation 4 has neglected any internal excitation of the parent. Although we have no way of ascertaining the internal excitation in the CH_3 at 1400 K we estimate that the methyl radicals should contain ~6 kcal/mole of vibrational energy prior to supersonic expansion, with most of this residing in the low frequency ν_2 umbrella mode. Chen *et.al.* have reported the complete vibrational relaxation of allyl radical produced under similar conditions[34] and even partial relaxation would leave the nascent methyl radicals with only 1-2 kcal/mole of vibrational energy on average. The maximum of the translational energy distribution, 28 kcal/mole, extends to the allowed thermodynamic limit for the formation of $CH_2(a^1A_1)$ + $H(^2S)$. Although the fastest CH_2 fragments overlap with the slowest CH_3 fragments from acetone in the *m/e*=12-14 spectra, the H-atom TOF spectrum and the angular distribution (Figure 8) allow sensitivity to the $P(E_T)$ maximum. We are confident, therefore, that the $P(E_T)$ does not have a significant contribution beyond 28 kcal/mole. Owing to high time dependent background at small laboratory angles,

Θ_{lab}=7.5° was the minimum angle at which TOF data was recorded. Based on the kinematics, CH_2 photofragments with less than 7 kcal/mole of translational energy could not be detected. Fortunately, the H-atom TOF spectra provides reliable information about the $P(E_T)$ down to 1.5 kcal/mole.

The laboratory angular distribution for the CH_2 fragments, monitored at *m/e*=12, is shown in Figure 8. Each point represents several individual measurements corrected for the laser power and the error bars are one standard deviation of the data. The low time dependent background from the pulsed valve at *m/e*=12 (C^+) made it the preferable mass to detect. The laser was polarized in the plane of the detector and along the molecular beam axis. For each measurement the total TOF profile was integrated with a scaler and the laser off signal was subtracted from the laser on signal at alternate shots. Since the TOF spectrum at *m/e*=12 involves contributions from both methyl radical and acetone photodissociation, the acetone signal needed to be carefully taken into account. In order to do this counts were taken at angles Θ_{lab}>20° where only the acetone contribution was present. Using the $P(E_T)$ for CH_3 from acetone and an isotropic dissociation as has been observed previously, the angular distribution for these fragments[28,29] was simulated using the forward convolution program. The simulation was then normalized to the measured signal at large laboratory angles and then the acetone contribution subtracted from the *m/e*=12 signal. TOF spectra taken at *m/e*=15 provided confirmation of the acetone angular distribution. It should be noted that given the large isotropic recoil of the CH_3 fragments from acetone photodissociation, the angular distribution is almost invariant over the range of interest. The *center-of-mass* product angular distribution is given by,

$$P(\theta) = \frac{1}{4\pi}\{1 + \beta P_2(\cos\theta)\} \tag{5}$$

where β is the anisotropy parameter and is equal to 2 if the transition moment and the dissociating bond are parallel and -1 if they are perpendicular in the limit of prompt recoil.[35] Shown in Figure 6 are three simulated laboratory angular distributions using the determined

$P(E_T)$ and anisotropy parameters of β=0.0, -0.5, and -1.0 corresponding to isotropic and increasingly perpendicular dissociations. From a best fit to the experimental angular distributions an anisotropy parameter of β=-0.9±0.1 has been determined. A negative β parameter was confirmed independently by rotating the polarization of the laser and observing the *m/e*=1 signal although the low signal-to-noise ratio precluded an accurate quantitative measurement.

IV. Discussion

A. Laser Polarization Dependence

At 193.3 nm methyl radical is excited to the *dissociative continuum* above the barrier along the C-H bond dissociation coordinate. Even at excitation energies below this barrier the CH_3 lifetime is subpicosecond. Kelly and co-workers have determined predissociation lifetimes of the CH_3 origin band to be <82fs[12] and the [1000] state was found to have a lifetime of ~13fs which is comparable to the C-H stretching frequency.[13] By nature of the continuum excitation at 193.3 nm the dissociation should occur with extreme rapidity. It is therefore unlikely that internal conversion could compete effectively with dissociation from the B-state and the observed anisotropy indicates that the dissociation is direct. The measured β=-0.9±0.1 indicates that the transition dipole moment lies perpendicular to the C-H bond which is consistent with the initial excitation of the out-of-plane p_z orbital on the carbon to a 3s Rydberg orbital. This represents the first measurement of the photofragment anisotropy for methyl radical dissociation from the B-state. Although the dissociation is much faster than rotation of the parent molecule any motion that contributes a velocity component perpendicular to the C-H bond will diminish the observed anisotropy. This effect would be particularly salient if the methyl radical dissociates from a range of non-planar geometries. Using the expression, $\beta=2P_2(\Theta)$, where Θ represents the angle between the C-H bond and the dipole moment operator this range can be calculated. On average the methyl would have to dissociate from geometries 10° from planarity with $75^o<\Theta<90^o$ coinciding to the spread in the measured anisotropy (-0.8 to -1.0). Any umbrella motion originating from either the transition at 193.3 nm or a hot band absorption of radicals already possessing ν_2 excitation would result in a

range of dissociations from non-planar geometries.

B. Product Translational Energy Distribution

The barrier on the B-state arises from a "de-Rydbergization" of the 3s orbital initially localized on the carbon as it evolves into a σ^* orbital on the C-H bond, and eventually to a 1s orbital on the departing hydrogen atom. The disposal of available energy into translation of the photofragments should be dominated by the repulsive interaction as the excited state develops σ^* character in the C-H bond. Given the 6.29 kcal/mole barrier height[13] and the 12.7 kcal/mole exoergicity of the reaction to form $CH_2(a^1A_1)$ + H, the total exit barrier is ~19 kcal/mole. If ground state methylene is produced then the exit barrier is increased by the magnitude of the singlet triplet splitting and is therefore ~28 kcal/mole. For a dissociation involving the cleavage of a single bond the fraction of the exit barrier appearing in translation can be estimated by using an impulsive model.[36] With the soft fragment impulsive model ~98% of the exit barrier would be expected to appear in product translation.[37] In fact, this partitioning was predicted earlier by Yu *et al.*[2] and is intuitively reasonable since the light H-atom should not effectively couple its impulse into the CH_2 vibrational degrees of freedom. Furthermore, the near planarity of the B-state should not facilitate any rotational excitation of the methylene fragment and even if the methyl radical dissociated from non-planar geometries the very small exit impact parameters when an H-atom recoils from the C atom in CH_2 would still result in negligible CH_2 rotation. However, only ~15 kcal/mole on average is observed in translation. This corresponds to only 80% and 54% of the exit barrier for singlet and triplet methylene respectively indicating substantial internal excitation. If the dissociation is prompt, as supported by the exhibited photofragment anisotropy, and there is little interaction in the exit channel, then the internal energy distribution may be determined by the change in $R_{C\text{-}H}$ and θ_{HCH} between the CH_3 and the free CH_2. Although there is little change in the C-H bond length, there is a substantial change in the HCH bond angle. The methyl radical is of D_{3h} symmetry and θ_{HCH}=120°, while for $CH_2(a^1A_1)$ θ_{HCH}=102.4° and for $CH_2(X^3B_1)$ θ_{HCH}=134°. Although Dixon and co-workers have now concluded[15] that vibrationless singlet methylene is produced from methyl radical photodissociation at 216 nm (rather than $CH_2(X^3B_1)$

with 0-3 quanta in ν_2 excitation[3]), the present results indicate that singlet or triplet methylene are formed with copious internal energy. According to the measured translational energy distribution there would be *no $CH_2(X^3B_1)$ containing less than 8 kcal/mole of internal energy*, with most $CH_2(X^3B_1)$ fragments possessing 23.1 kcal/mole of internal energy on average. If, however, singlet methylene were the dissociation product it would contain ~13 kcal/mole of internal energy on average. Since the $P(E_T)$ extends to the thermodynamic limit there is a finite probability of forming vibrationless $CH_2(a^1A_1)$. Although the slope of the $CH_2(^1A_1)$ bending coordinate in the exit channel is not as steep as for $CH_2(X^3B_1)$ the breadth of the $P(E_T)$ suggests that the methyl radical samples a wide range of dissociative geometries. The absorption to the dissociative continuum is sufficiently far above the barrier to be relatively insensitive to the least motion pathway. Therefore, the observed $P(E_T)$ is certainly consistent with excitation in the other vibrational modes of the methylene. We conclude that the most likely dissociation product is $CH_2(a^1A_1)$ which is consistent with theoretical prediction.[2] In addition, wavepacket calculations on empirical potential energy surfaces find that formation of triplet methylene requires an anomalously large coupling between the ground and excited state surfaces.[38]

In light of the vibrationless $CH_2(a^1A_1)$ observed by Dixon and co-workers, one must ask why the resulting energy distribution at 193.3 nm is so different. The apparent discrepancy can be expained by considering the fundemental differences between the dynamics imposed by a continuum compared to a tunneling dissociation. Since methyl radical at 216 nm is excited to the band origin only zero point motion will contribute to the range of dissociative geometries. In addition, the dissociation barrier depends on the HCH angle and to an extent, so should the tunneling rate. Therefore, the methyl radical excited at 216 nm dissociates from an extremely narrow range of geometries which are biased toward HCH angles <120°. These out going trajectories run close to the minimum on the $CH_2(a^1A_1)$ bending potential (θ_{HCH}=102°) and therefore result in predominately vibrationless nascent products. At 193.3 nm there is no *a priori* reason to believe that the dissociation should be constrained to a small dispersion about the CH_3 equilibrium geometry. The range of dissociation geometries should be determined, in part, by the initial motion of the nuclei

upon excitation to the continuum. Therefore, there is no preference for outgoing trajectories to sample that part of the potential energy surface that corresponds to a least motion pathway. If the dissociation proceeds through a broad range of coordinate space a high degree of internal excitation in the CH_2 products should result.

V. Concluding Remarks

In conclusion, the photodissociation of methyl radical at 193 nm has been studied using photofragment translational spectrocopy. The only single photon products observed were CH_2 and H and is the first time that the branching ratio between H-atom and H_2 elimination from CH_3 photochemistry has been directly determined. Although we cannot unambiguously assign the spin-state of the methylene product, we believe, in light of the translational energy distribution and overwhelming theoretical work, that $CH_2(a^1A_1)$ is the predominate dissociation product. Since a definitive determination of the methylene spin-state has yet to be made at any wavelength, any measurement to this end would represent an important contribution to the further elucidation of methyl radical photochemistry. The breadth of internal energy measured in this experiment is consistent with the dissociation occuring from a wide range of dissociative geometries. Work is currently in progress to examine the B-state photochemistry in greater detail with a higher resolution TOF technique and at energies below the excited state barrier.

Acknowledgments. The Authors would like thank Dr. A. Suits for many helpful discussions. They would also like to acknowledge Dr. D. Stranges and Dr. M. Stemmler for their help with the pyrolytic radical source. This work was supported by the Director, Office of Energy Research, Office of Basic Energy Sciences, Chemical Sciences Division of the U.S. Department of Energy under Contract No. DE-ACO3-76SF00098.

References

1. M. T. Macpherson, M. J. Pilling, and M. J. C. Smith, *J. Phys. Chem.*, **89**, 2268 (1985); J. E. Butler, L. P. Gross, M. C. Lin, and J. W. Hudgens, *Chem. Phys. Lett*, **63**, 104 (1979); M. R. Berman and M. C. Lin, *J. Chem. Phys.*, **81**, 5743 (1984); S. Zabarnick, J. W. Fleming, and M. C. Lin, *J. Chem. Phys.*, **85**, 4373 (1986); M. Aoyagi, R. Shepard, A. F. Wagner, T. H. Dunning, Jr., and F. B. Brown, *J. Phys. Chem.*, **94**, 3236 (1990); B. R. Brooks, H. F. Schaefer, III, *J. Chem. Phys.*, **67**, 5146 (1977).

2. P. Chen, S. D. Colson, and W. A. Chupka, *Chem. Phys. Lett.*, **147**, 466 (1988).

3. S. H. S. Wilson, M. N. R. Ashfold, and R. N. Dixon, *Chem. Phys. Lett.*, **222**, 457 (1994).

4. H. T. Yu, A Sevin, E. Kassab, and E. M. Evleth, *J. Chem. Phys.*, **80**(5), 2049 (1984).

5. G. Herzberg and J. Shoosmith, *Canad. J. Phys.*, **34**, 523 (1956).

6. G. Herzberg, *Proc. Roy. Soc.*, **A 262**, 291 (1961).

7. A. B Callear and M. P. Metcalfe, *Chem. Phys.*, **14**, 275 (1976).

8. C. Ye, M. Suto, and L. C. Lee, *J. Chem. Phys.*, **89** (5), 2797 (1988).

9. P. D. Lightfoot, S. P. Kirwan, and M. J. Pilling, *J. Phys. Chem.*, **92**, 4938 (1988).

10. J. E. Baggott, M. Brouard, M. A. Coles, A. Davis, P. D. Lightfoot, M. T. Macpherson, and M. J. Pilling, *J. Phys. Chem.*, **91**, 317 (1987).

11. C. Kassner, P. Heinrich, F. Stuhl, S. Couris, and S. Haritakis, *Chem. Phys. Lett.*, **208**, 27 (1993).

12. S. G. Westre, P. B. Kelly, Y. P. Zhang, and L. D. Zeigler, *J. Chem. Phys.*, **94**(1), 270 (1991).

13. S. G. Westre, T. E. Gansberg, P. B. Kelly, and L. D. Zeigler, *J. Phys. Chem.*, **96**, 3610 (1992).

14. P. Botschwina, E. Schick, and M. Horn, *J. Chem. Phys.*, **98**, 9215 (1993).

15. S. H. S. Wilson, J. D. Howe, K. N. Rosser, M. N. R. Ashfold, and R. N. Dixon, *unpublished results.*

16. The apparent high resolution of the TOF spectrum in ref. 3 could not be reproduced in this laboratory using the forward convolution technique.

17. S. H. S. Wilson, M. N. R. Ashfold, and R. N. Dixon, *J. Chem. Phys.*, in press (1994).

18. Y. T. Lee, J. D. McDonald, P. R. LeBreton, and D. R. Herschbach, *Rev. Sci. Instrum.*, **40**, 1402, (1969).

19. S. W. North, C. A. Longfellow, and Y. T. Lee, *J. Chem. Phys.*, **99**, 4423 (1993).

20. D. Proch and T. Trickl, *Rev. Sci. Instrum.*, **60**, 713 (1989).

21. D. W. Kohn, H. Clauberg, and P. Chen, *Rev. Sci. Instrum.*, **63**(8), 4003 (1992); H. Clauberg, D. W. Minsek, and P. Chen, *J. Am. Chem. Soc.*, **114**, 99 (1992); H. Clauberg and P. Chen, *J. Am. Chem. Soc.*, **113**, 1445 (1991).

22. T. G. DiGiuseppe, J. W. Hudgens, and M. C. Lin, *J. Phys. Chem.* **86**, 36 (1982); G. N. Robinson, G. M. Nathanson, R. E. Continetti, and Y. T. Lee, *J. Chem. Phys.* **89**, 6744 (1988); C. Yamada, E. Hirota, and K. Kawaguchi, *J. Chem. Phys.*, **75**, 5256 (1981).

23. R. E. Continetti, Ph.D. thesis, University of California, Berkeley, 1989; R.E. Continetti, B. A. Balko, and Y. T. Lee, *Chem. Phys. Lett.* **184**, 400 (1991); R. E. Continetti, B. A. Balko, and Y. T. Lee, *J. Chem. Phys.* **93**, 5719 (1990).

24. B. A. Balko, Ph.D. thesis, University of California, Berkeley, 1991; B. A. Balko, J. Zhang, and Y. T. Lee, *J. Chem. Phys.* **94**, 7958 (1991).

25. A. M. Wodtke, Ph.D. thesis, University of California, Berkeley, 1986; X. Zhao, Ph.D. thesis, University of California, Berkeley, 1988; X. Zhao, G. M. Nathanson, and Y. T. Lee, *Acta Physico-Chim. Sinica*, **8**, 70 (1992).

26. R. Renaud and L. C. Leitch, *Can. J. Chem.* **32**, 545 (1954).

27. G. A. Gaines, D. J. Donaldson, S. J. Strickler, and V Vaida, *J. Phys. Chem.*, **92**, 2762 (1988).

28. S. W. North, D. A. Blank, C. A. Longfellow, and Y. T. Lee, *unpublished results.*

29. K. A. Trentelman, S.H. Kable, D. B. Moss, and P. L. Houston, *J. Chem. Phys.*, **91**, 7498 (1989).

30. S. W. North, P. Chu, and Y. T. Lee, *XIVth International Symposium on Molecular Beams,* Asilomar, CA., 1992.

31. D. R. Stull and H. Prophet et al., *JANAF Thermochemical Tables*, 2nd ed., Natl. Stand. Ref. Data Ser. Natl. Bur. Stand. (U.S. GPO, Washington, D.C., 1971); S. Zabarnick, J. W. Fleming, and M. C. Lin, *J. Chem. Phys.* **85**, 4373 (1986).

32. S. W. Benson, *Thermochemical Kinetics*, 2nd ed. (Wiley, New York, 1976).

33. I. Shavitt, *Tetrahedron*, **41**(8), 1531 (1985) and references therein.

34. J. A. Blush, D. W. Minsek, and P. Chen, *J. Phys. Chem.* **96**, 10150 (1992).

35. R. N. Zare, Ph.D. Harvard University, 1964; R. N. Zare, *Mol. Photochem.*, **4,** 1 (1974).

36. G. E. Busch and K. R. Wilson, *J. Chem. Phys.* **56**, 3626 (1972).

37. The expression for the fraction of the available energy partitioned into translation is given by, $f_T=[\mu_{C\text{-}H}/\mu_{CH2\text{-}H}]$, where μ is the reduced mass.

38. R. N. Dixon, *unpublished results.*

Figure Captions

Figure 1: Energy level diagram for methyl radical showing the energetically accessible dissociation channels for 193.3 nm excitation.

Figure 2: Mass spectra of the molecular beam of <1% di-tertbutyl peroxide in He taken with the pyrolytic nozzle at (a) room temperature (*heat off*) and (b) 1400K (*heat on*).

Figure 3: TOF spectra at a laboratory angle of 7.5^{o} for (a) *m/e*=15(CH_3^+) (b) *m/e*=14(CH_2^+) (c) *m/e*=13(CH^+) and (d) *m/e*=12 (C^+). The open circles represent data. The dotted line is the contribution from acetone dissociation, the dashed line is the contribution from CH_3 dissociation using the $P(E_T)$ in Figure 4, and the solid line is the total fit to the data.

Figure 4: Center-of-mass translational energy distribution used to fit the data in Figures 3,5, and 6. Arrows indicate the thermodynamic maximum available energies for formation of singlet and triplet methylene.

Figure 5: TOF spectra of *m/e*=12 (CH_2^+) at laboratory angles of (a) 10° and (b) 14°. The open circles represent data. The dotted line is the contribution from acetone dissociation, the dashed line is the contribution from CH_3 dissociation using the $P(E_T)$ in Figure 4, and the solid line is the total fit to the data.

Figure 6: TOF spectrum of *m/e*=1 (H^+) at a laboratory angle of 90°. The open circles represent data with the time-dependent background subtracted. The solid line represents the forward convolution fit using the $P(E_T)$ in Figure 4.

Figure 7: TOF spectrum of *m/e*=2 (H_2^+) at 90°. The open circles are the data with the laser on and the solid line is the data taken with the laser off.

Figure 8: Laboratory angular distribution of the CH_2 photofragments detected at *m/e*=12(C^+) with the laser polarized at 0°. The lines are simulated angular distributions assuming three different values of the anisotropy parameter (see text).

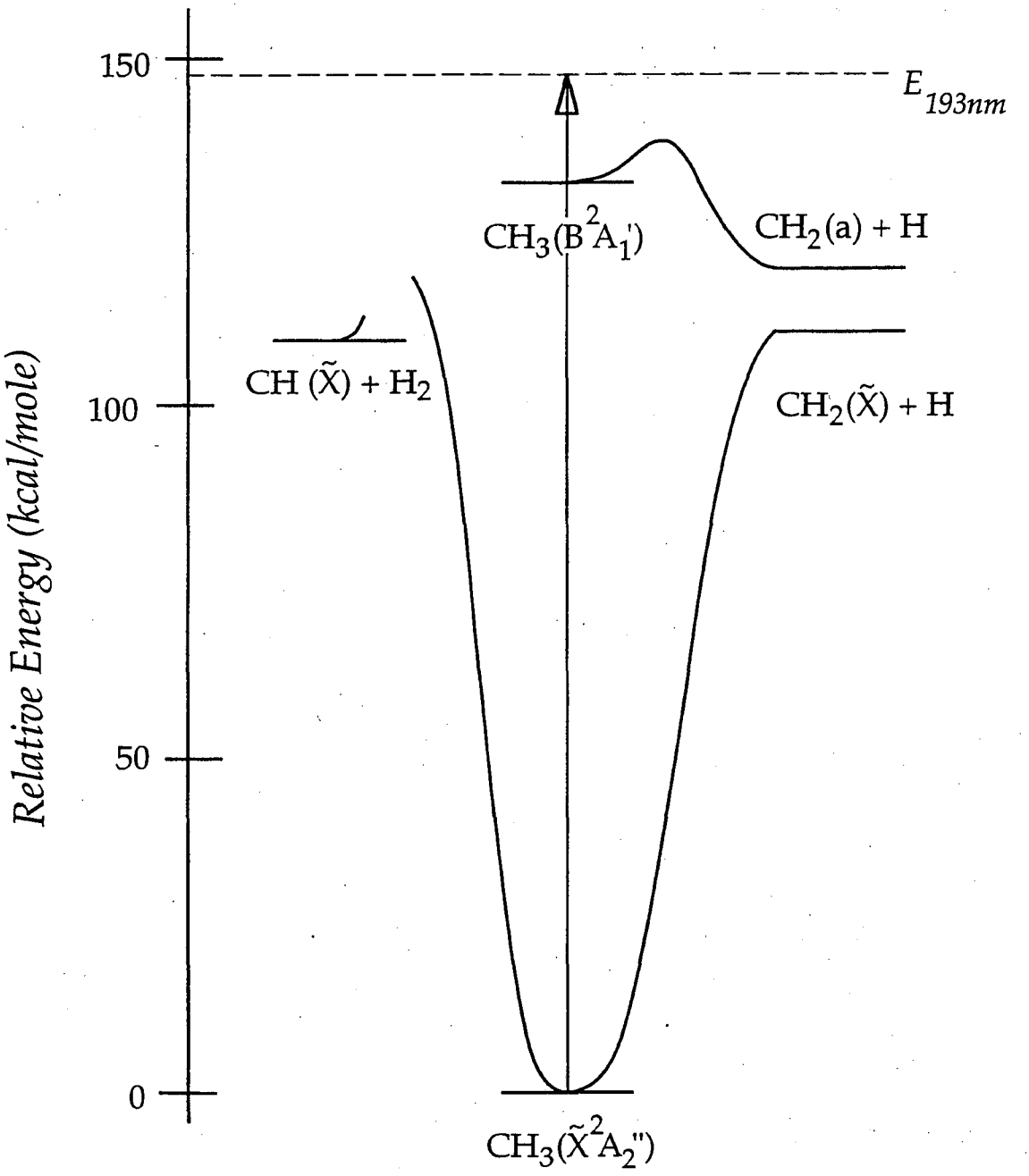
150
100
50
0
Relative Energy (kcal/mole)
E_{193nm}
$CH_3(B^2A_1')$
$CH_2(a) + H$
$CH\ (\tilde{X}) + H_2$
$CH_2(\tilde{X}) + H$
$CH_3(\tilde{X}^2A_2'')$

Figure 1

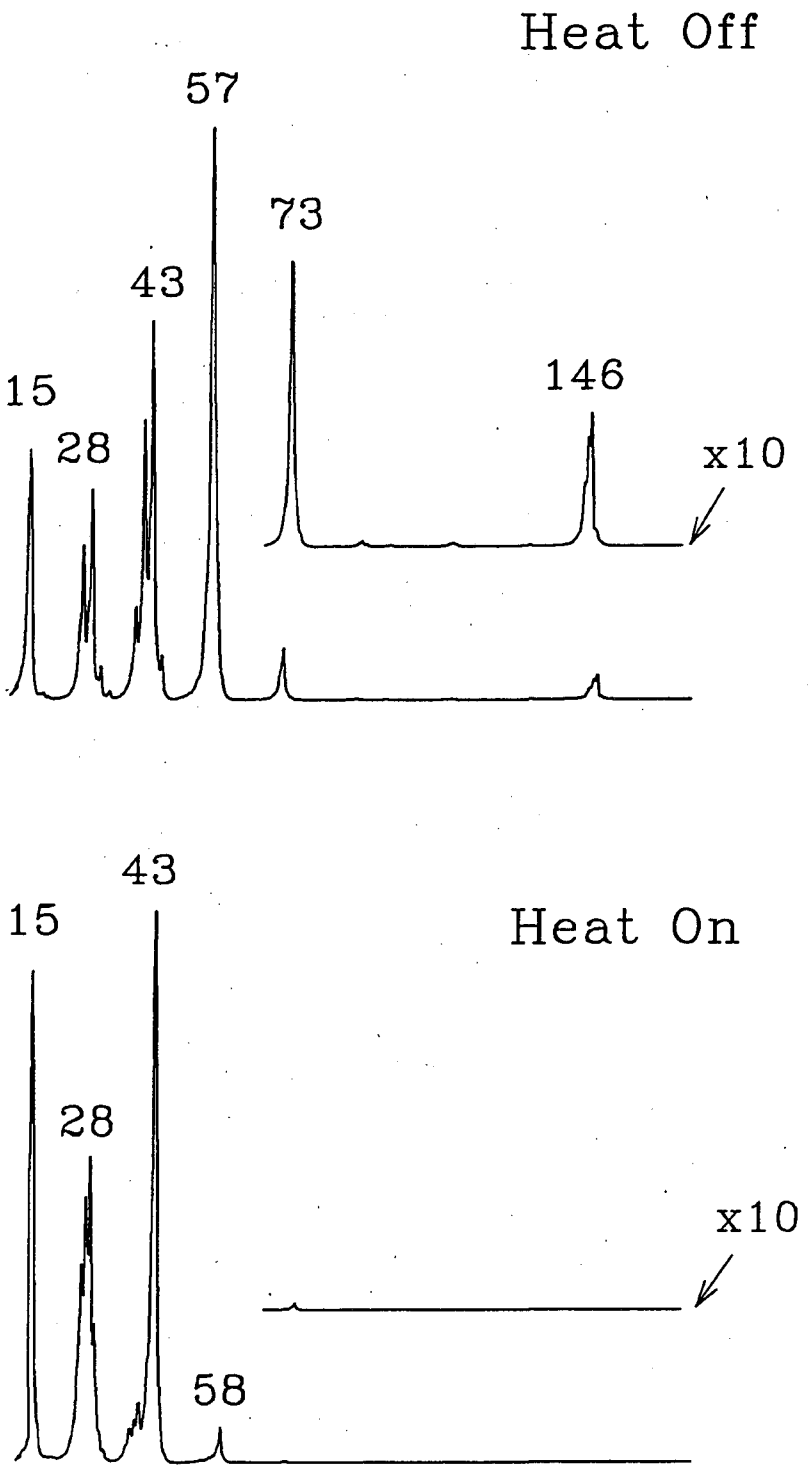

Figure 2

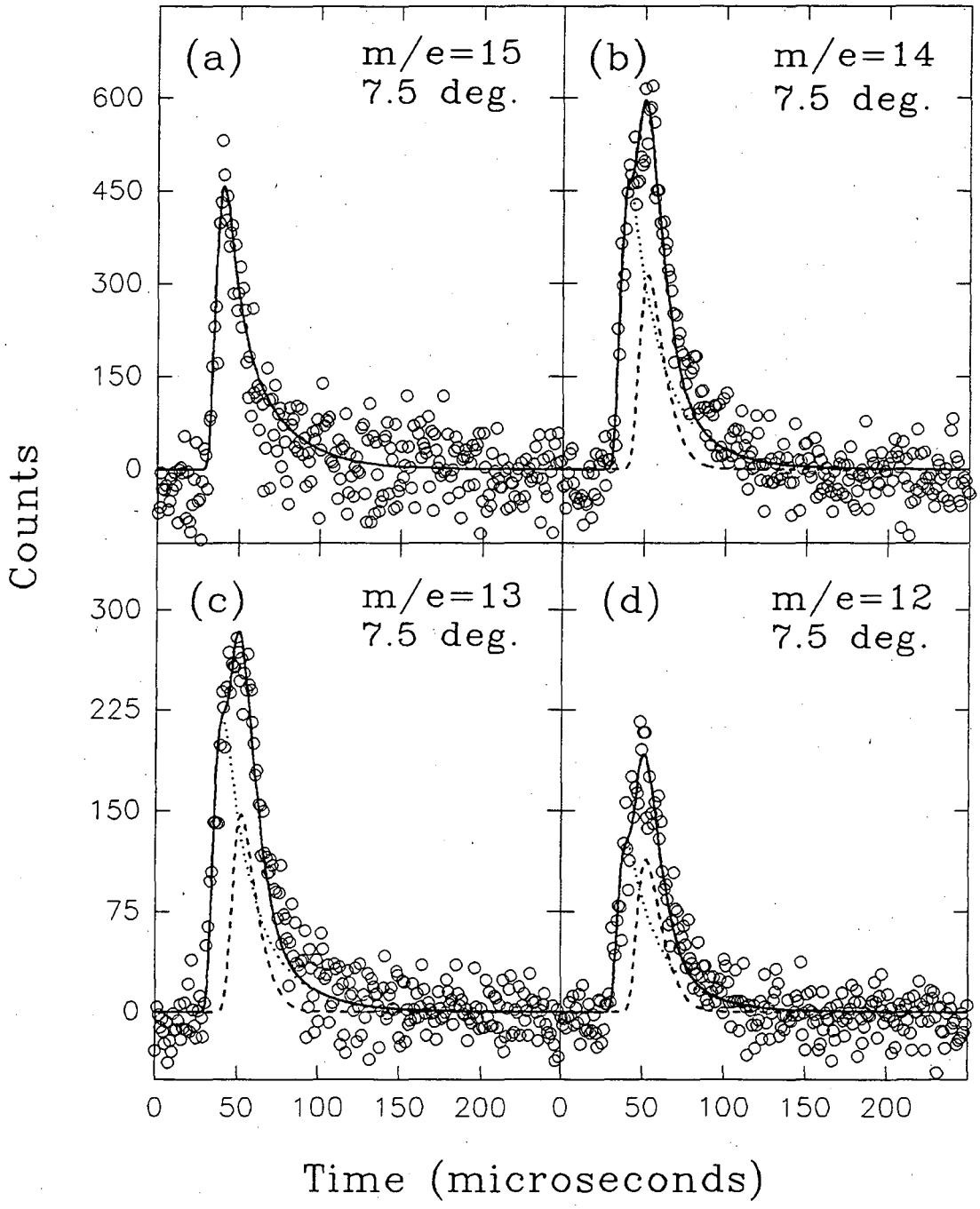
(a)
m/e=15
7.5 deg.
(b)
m/e=14
7.5 deg.
(c)
m/e=13
7.5 deg.
(d)
m/e=12
7.5 deg.
Counts
600
450
300
150
0
300
225
150
75
0
0
50
100
150
200
Time (microseconds)

Figure 3

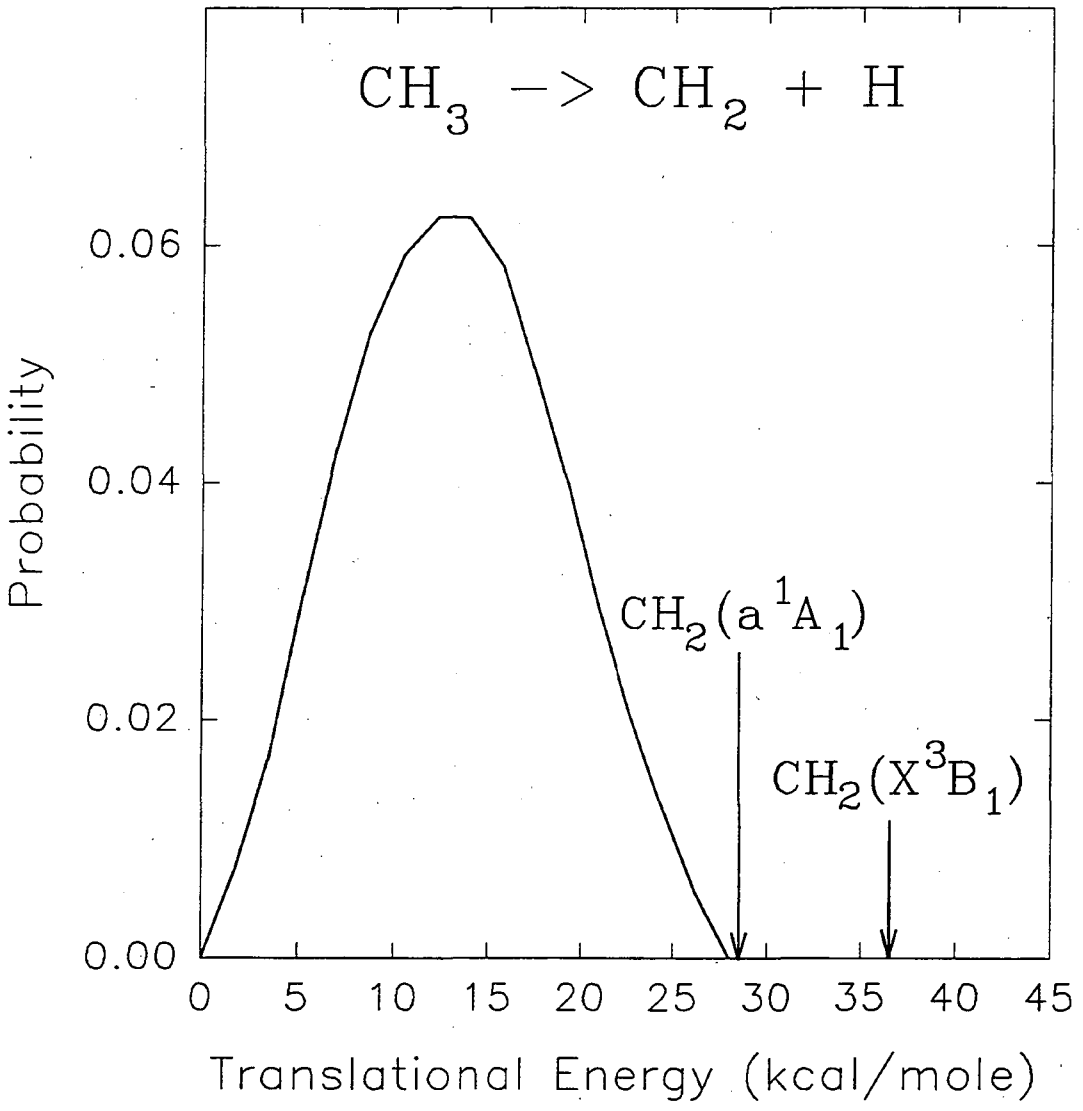
CH3 -> CH2 + H
0.06
0.04
0.02
0.00
Probability
CH2(a 1A 1)
CH2(X 3B 1)
0
5
10
15
20
25
30
35
40
45
Translational Energy (kcal/mole)

Figure 4

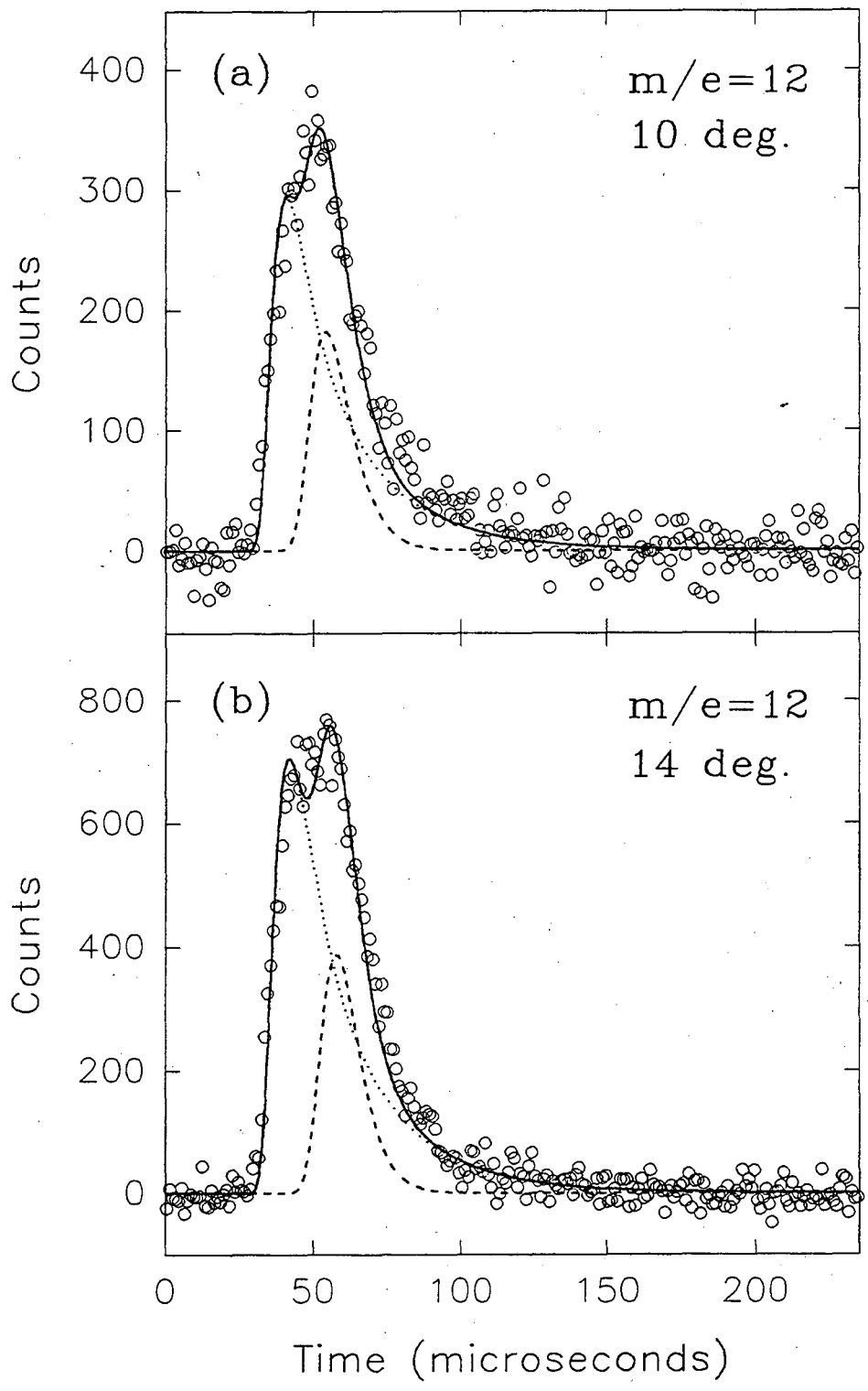
(a)
m/e=12
10 deg.
400
300
200
100
0
Counts
(b)
m/e=12
14 deg.
800
600
400
200
0
Counts
0
50
100
150
200
Time (microseconds)

Figure 5

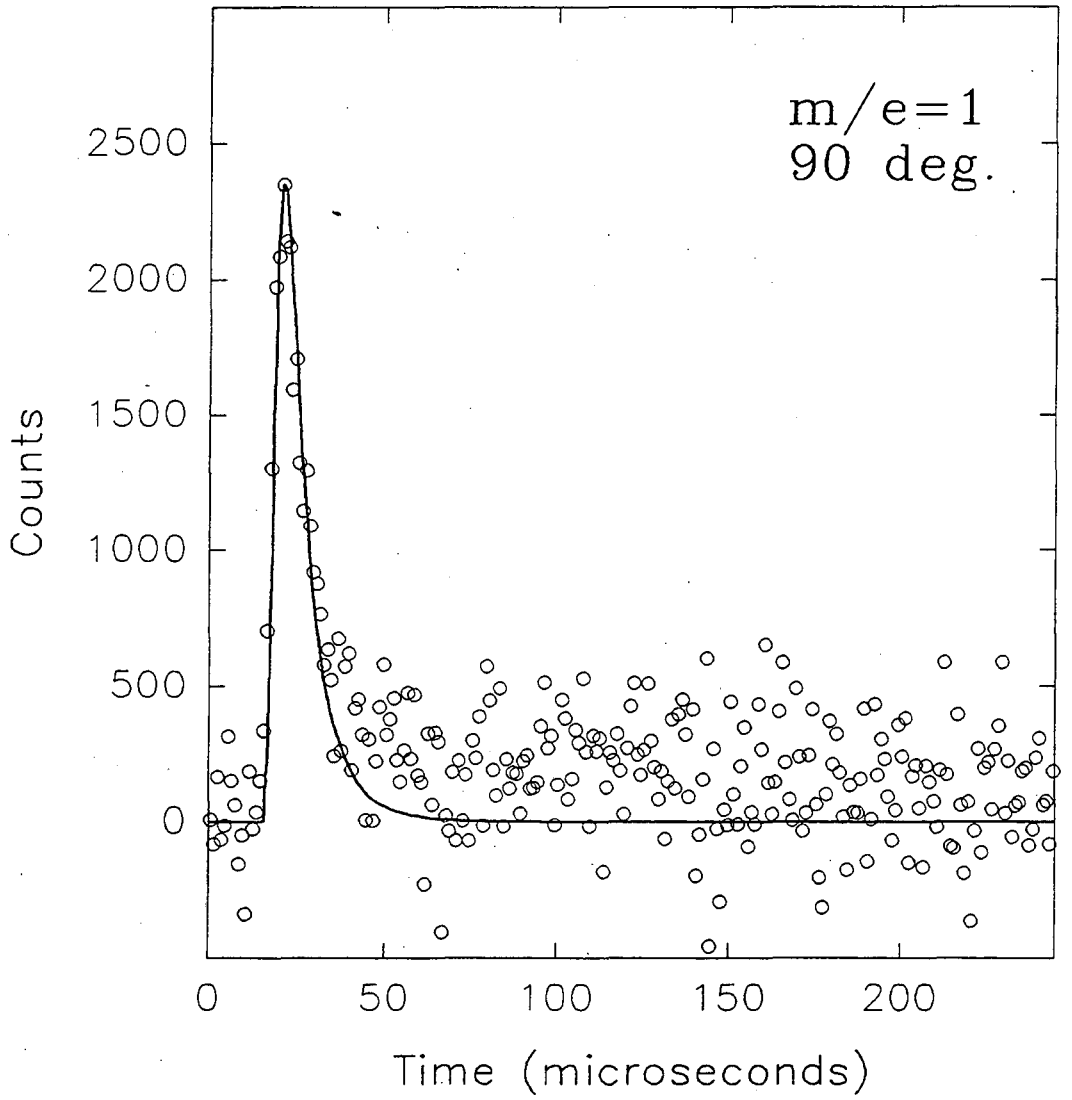
m/e=1
90 deg.
2500
2000
1500
1000
500
0
Counts
0
50
100
150
200
Time (microseconds)

Figure 6

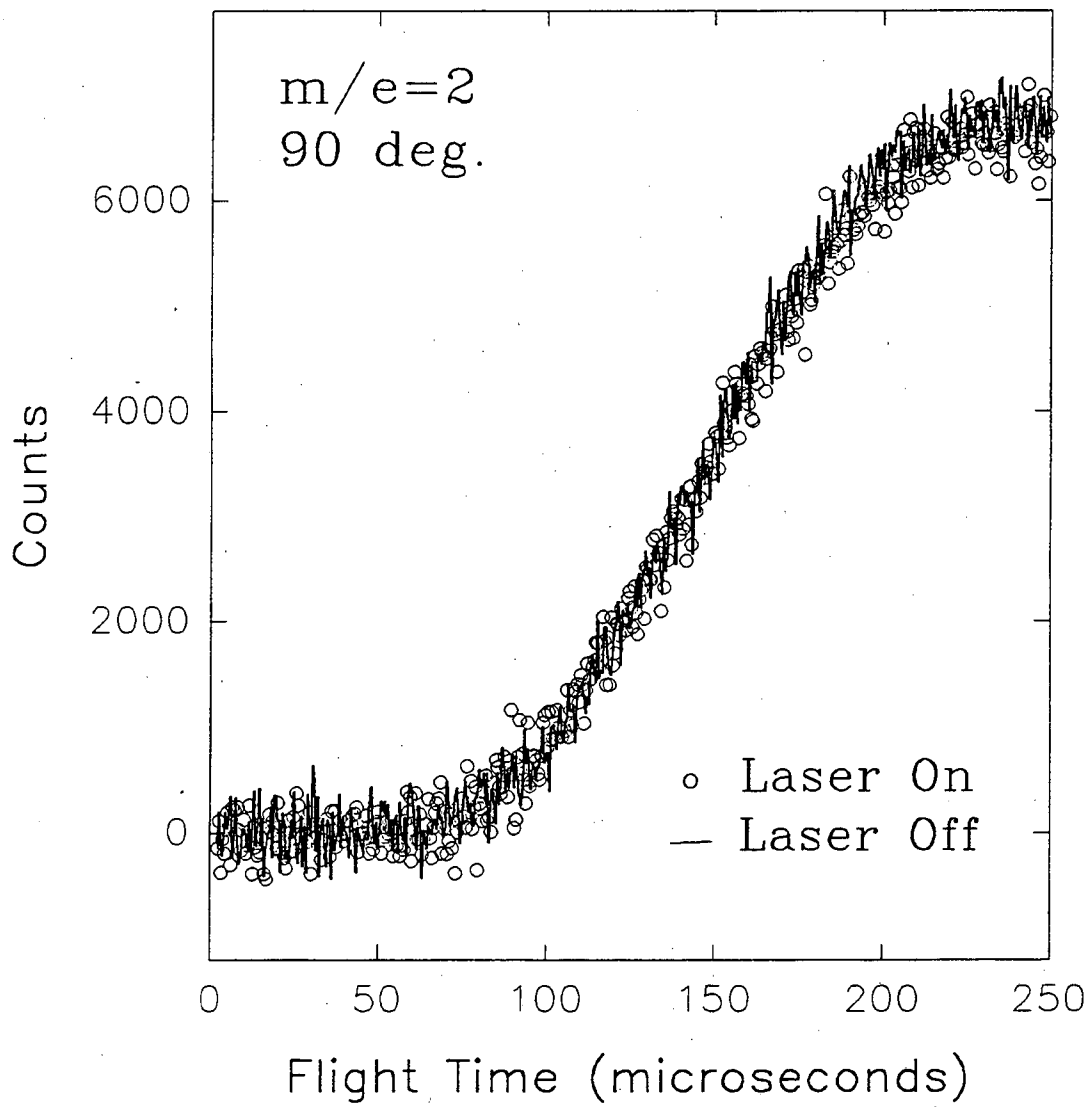
m/e=2
90 deg.
6000
4000
2000
0
Counts
Laser On
Laser Off
0
50
100
150
200
250
Flight Time (microseconds)

Figure 7

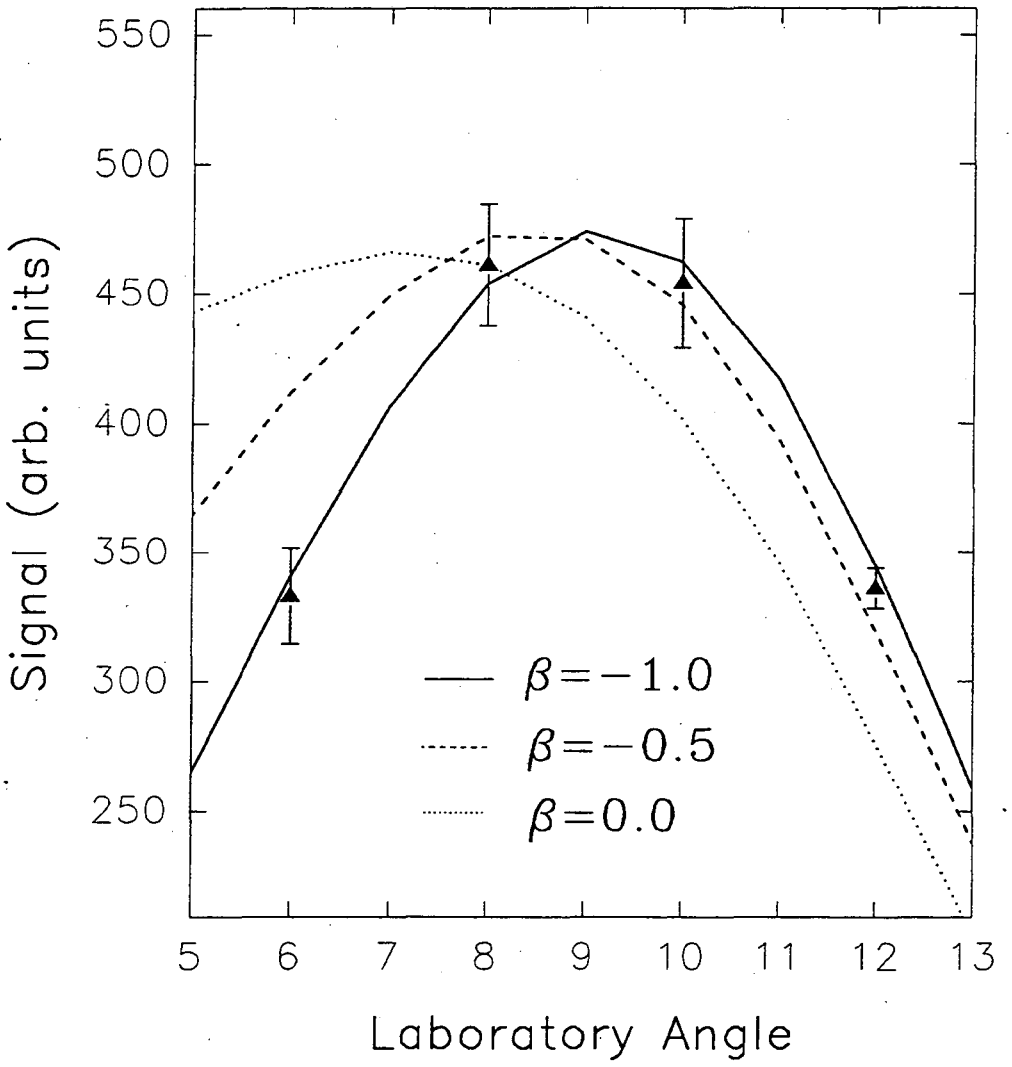
550
500
450
400
350
300
250
Signal (arb. units)
5
6
7
8
9
10
11
12
13
Laboratory Angle
$\beta=-1.0$
$\beta=-0.5$
$\beta=0.0$

Figure 8

LAWRENCE BERKELEY LABORATORY
UNIVERSITY OF CALIFORNIA
TECHNICAL INFORMATION DEPARTMENT
BERKELEY, CALIFORNIA 94720